PAPER AAS 95-307

DESIGN OF HIGH-ACCURACY MULTIPLE FLYBY TRAJECTORIES USING CONSTRAINED OPTIMIZATION

Dennis V. Byrnes, Larry E. Bright

Jet Propulsion Laboratory
California Institute of Technology
Pasadena, California 91109

AAS/AIAA Astrodynamics Specialist Conference

HALIFAX, NOVA SCOTIA, CANADA **14-17 AUGUST 1995**

AAS Publications Office, P.O. Box 28130, San Diego, CA 92198

AAS 95-307

DESIGN OF HIGH-ACCURACY MULTIPLE FLYBY TRAJECTORIES USING CONSTRAINED OPTIMIZATION

Dennis V. Byrnes*
Larry E. Bright+

Over the past two decades the extremely difficult problem of efficiently finding optimal trajectories with multiple gravitating bodies has frequently been addressed. The technique described in this paper provides distinct advantages over previous formulations. The trajectories are numerically integrated without a requirement for solutions of multiple boundary value problems. A novel method of splitting the trajectory into independent legs with each leg independently specified by any convenient set of parameters is described. Any of these parameters may then be subject to constraints. The nonlinear constrained optimization problem is then solved as a sequence of linear problems, Examples for several deep space missions are given.

INTRODUCTION

The extremely difficult problem of efficiently finding optimal trajectories that involve close flybys of multiple gravitating bodies has been addressed by many investigators over the past two decades using a variety of methods (Ref. 1 -4). Although the method and particular formulation described in this paper are in part directly related to several of those methods, several new advances have been made. A novel way of splitting the trajectory into legs, removal of the time consuming and sometimes numerically unstable requirement of solving many boundary value problems, and the continued advance in computing capability of modern computer workstations have allowed for significant improvements in speed, ease of use, numerical stability and accuracy of the resulting trajectory design.

METHOD

Optimal trajectories are determined starting from a specified state vector, or from launch or flyby body conditions which are consistent with a specified set of constraints and a specified flyby body sequence. optionally, in the case of interplanetary trajectories, certain arrival conditions may also be specified, Tile trajectory optimization technique described in this paper provides several distinct advantages over previous formulations.

First, fully numerically integrated trajectory modeling is used. That is, no approximations to the trajectory are made and the inclusion of any level of complicated force

* Member Technical Staff, Jet Propulsion Laboratory, California Institute of Technology; Member AIAA; Member AAS
+ Member Technical Staff, Jet Propulsion Laboratory, California Institute of Technology

models desired is allowed. Trajectory modeling is based on numerical integration of the equations of motion of a point-mass spacecraft subject to gravitational accelerations. Additional effects modeled are impulsive and/or finite motor burns and solar pressure. The gravitational models include, in addition to the inverse-square acceleration due to the primary central body, point-mass gravitational accelerations due to any combination of sun, planets, satellites, asteroids or comets plus acceleration due to the oblateness of the central body,

Second, only trajectory propagation is used so there is no requirement for solutions of multiple boundary value problems as intermediate steps before optimization. This is accomplished by the novel method of splitting the trajectory into independent legs, which are then subjected to constrained optimization. Initially these legs will, in general, not be continuous in either position or velocity. Consequently none of the numerical problems associated with the solving of a series of boundary problems will arise. Position continuity in the final trajectory is achieved by imposing constraints on the optimization.

Third, each of the trajectory legs may be specified by any convenient set of parameters particularly useful for that leg, Any of these parameters may then be subject to constraints, Trajectory constraints may include flyby altitudes, b-plane angles, latitudes, times of closest approach to flyby bodies, inclinations or essentially any other orbital parameter with respect to either the primary or secondary body including the Cartesian state vector. There may also be constraints on maneuvers such as time, direction, location and mode of execution. Any of these constraints may be equality, inequality or bounds constraints, and will, of course, be closely related to mission operations requirements and science objectives.

Fourth, the solution to the nonlinear optimization problem is found by solving a sequence of linear problems that converges to the optimal nonlinear solution. The method of solution used is a parameter optimization algorithm based on a series of linearization of the "real" highly nonlinear problem. The optimization algorithm changes the independent variables (a series of estimated states along the trajectory, usually at flybys) on successive iterations to reduce the cost function (total ΔV). Due to the complexity of some problems, it may sometimes be necessary for the user to actively control the optimization process to achieve convergence. This is particularly true when a new problem is addressed with only some very approximate guesses available to specify the problem. A variety of control procedures are available for these situations. In general, though, the robustness of this formulation requires little or no user interaction with the optimization once a feasible problem has been posed.

Finally, although it is not the subject of this paper, our software implementation of this method (in a new program called CAT() – Computer Algorithm for Trajectory Optimization) makes use of FORTRAN 90, modern techniques of object oriented programming, and extremely fast UNIX based workstation computers. The result is a very rapid and convenient way of producing very high precision, optimal trajectory designs.

OPTIMIZATION PROBLEM STRUCTURE

Trajectory Structure

A complete trajectory is broken up into a sequence of user-defined trajectory legs, The legs are contiguous in time. The boundary between two successive legs is referred to as a trajectory breakpoint, On each trajectory leg there is a unique distinguished point re-

ferred to as the control point for that leg. A set of 7 control point variables is defined at each control point by the user, One of the variables is an epoch and the remaining 6 are a parameterization of the spacecraft state (position and velocity) at that epoch. The specific parametrization of the state is chosen from a wide range of possibilities (numbering in the hundreds) separately for each trajectory leg.

The control point variables collectively, over all legs of the trajectory, determine the initial conditions for trajectory propagation and are a subset of the independent variables for optimization. Any leg of the trajectory may optionally have an additional three independent variables that are associated with a maneuver at the beginning of the trajectory leg. These AV variables may be included in the independent variable set to impose constraints on them.

Breakpoints and control points occur in alternating fashion along a trajectory. For example, on a trajectory with n legs, they occur in the following order:

$$B_0, C_1, \mathbf{B}], C_2, \ldots . C_n, B_n,$$

where the B_i's are breakpoints and the C_i's are control points. The entire trajectory begins at the initial breakpoint B_0 and ends 'at the terminal breakpoint, B_n. This is shown schematically in Figure 1.

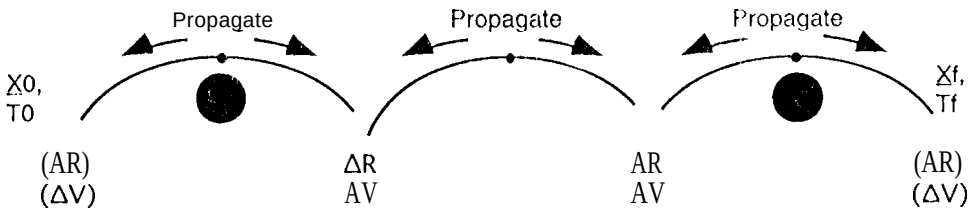

Figure 1. Trajectory Schematic (CATO)

By contrast, the method described in References 1 and 2 required the solution of a boundary value problem on each leg that required greater numerical complexity and computation time. This earlier method is shown schematically in Figure 2.

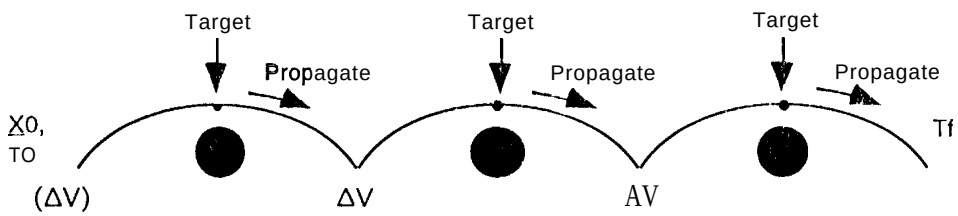

Figure 2. Trajectory Schematic (Earlier Method)

Trajectory Generation

On a given iteration of the optimization procedure, a trial trajectory must be generated from the current values of the independent variables. The legs of a trajectory are generated separately and independently. Each leg is the result of two trajectory propagations: first, a reverse (i. e., backwards in time) propagation from the control point for the

leg to the epoch of the starting breakpoint of the leg; second, a forward propagation from the control point to the ending breakpoint of the leg. The trajectory generation process is complete when all the trajectory legs have been determined in this way. Although the current implementation of CATO processes the legs sequentially, since the legs are independent this formulation is ideal for possible implementation using parallel processors.

At each trajectory breakpoint there is an "incoming" velocity, which results from forward propagation of the trajectory from the preceding control point, and an "outgoing" velocity, which results from reverse propagation of the trajectory from the succeeding control point. Thus, while the propagation procedure guarantees that a trajectory is continuous within a leg, there will, in general, be discontinuities in both position and velocity at the breakpoints between legs (see Figure 1). In order to achieve a final trajectory that is continuous in position, constraints are automatically imposed on the optimization requiring that position discontinuities at breakpoints be zero. Velocity discontinuities, on the other hand, cannot always be eliminated, since maneuvers may be physically necessary to fly the trajectory within the constraints. Within the available degrees of freedom, however, the user may choose to impose constraints requiring that velocity discontinuities at selected breakpoints be constrained to zero, even when this is not optimal.

Placement of Breakpoints and Control Points

For reasons that should be clear from the preceding discussion of trajectory generation, maneuvers that are subject to optimization may only occur at trajectory breakpoints, Thus, breakpoints will normally be placed at points on the trajectory where AV's are required or expected to be needed. Apart from this consideration, the placement of trajectory breakpoints is arbitrary.

The control point for a leg will usually occur between the epochs defining the bounding breakpoints of the leg. No such requirement is imposed by the CATO program however, and there are situations in which it can be very useful to place the control point outside this interval. This allows constraints to be imposed on a trajectory leg based on conditions that lie on a hypothetical extension of the trajectory leg beyond its actual limits. in a later section it will be seen, for example, that this feature can be used to target the Cassini *Orbiter* such that the Cassini *Probe* will meet certain constraints at its entry into Titan's atmosphere. Another natural use of this feature is for imposing planetary quarantine constraints on certain trajectory legs. In this situation it is desired to constrain the trajectory such that *if a certain maneuver fails to occur* the resulting trajectory must not impact (for example) the Earth. Apart from considerations such as these, control points may be placed arbitrarily by the user. In particular, a control point and a breakpoint may coincide.

A trajectory leg may contain zero, one or more flybys of gravitating bodies. In normal practice, trajectory breakpoints will be at or near the expected maneuver epochs, with at least one between significant gravity-assist flybys. A leg will typically contain one flyby; the control point for the leg will typically be placed at or near the periapsis of the flyby. None of these situations is in fact required by the method however. Note that non-zero maneuvers will in general occur at the initial breakpoint, B_0, and at the terminal breakpoint, B_n, if not otherwise constrained.

ITERATIVE SOLUTION OF THE OPTIMIZATION PROBLEM

The optimization problem is a highly nonlinear one due to the nonlinear nature of the multi-body equations of motion. The nonlinear problem is solved as the limiting case of a series of linear (or "linearized") problems. Each linearized problem is itself solved iteratively as a sequence of problems through a process called "re-weighting the cost function".

Thus, the method consists of a loop-within-a-loop structure, with the inner iteration controlling the re-weighting process and the outer iteration controlling the re-linearization process. When both iterations have converged, the "real" nonlinear problem with the "real" sum-of-magnitudes cost function has been solved.

The cost function that is minimized is the sum of the AV magnitudes. For numerical reasons, an indirect approach to computing this cost function is used. The cost function is:

$$\Delta V_{total} = w_1 \Delta V_1^2 + w_2 \Delta V_2^2 + \ldots + w_n \Delta V_n^2$$

where:
n = number of allowed maneuvers on the trajectory
ΔV_i = magnitude of the ith ΔV vector
and w_i = scale factor or "weight" associated with the ith maneuver

The w_i 's are initially set to the somewhat arbitrary value of 1.0. They are then adjusted in a series of automated "re-weighting" operations. When iterative re-weighting is finished, each weight equals

1 / (the corresponding ΔV)

or, expressed differently, the reciprocal of the weight equals the corresponding ΔV magnitude. The cost function, then, reduces to precisely

$$\Delta V_1 + \Delta V_2 + \ldots + \Delta V_n$$

i.e., the sum of the AV magnitudes, which is the"] eal" cost function to be minimized.

For each set of weights, the current linearized version of the trajectory optimization problem is solved by a utility linear- least-squares minimization package. When the re-weighting process converges, the resulting trajectory solution is used to determine a new linearization of the nonlinear problem; the re-weighting process is done on this new linearization, etc., until there is only a negligible change from one linearization to the next.

RESULTS

To illustrate the characteristics and performance of the computer software that implements the trajectory optimization method described in this paper, several examples are presented, These include: the trajectory for the orbital tour phase of the Galileo mission; a potential interplanetary transfer trajectory for the Cassini mission from Earth to Saturn with 4 intermediate planetary flybys; an example orbital insertion phase trajectory

for the Cassini mission that includes both the Probe and Orbiter trajectories to Titan; and a potential Stardust (proposed Discovery) mission trajectory that incorporates a flyby of comet Wild-2 and a return to Earth with collected dust samples. In addition to these examples, CATO will be used in the near future on several trajectory classes involving multiple lunar flybys to reach near-Earth asteroids and libration point orbits. Extensive use in the re-optimization of the Galileo orbital tour trajectory during ongoing mission operations is anticipated once successful injection into Jupiter orbit has been achieved on December 7, 1995. CATO will also be used for the detailed design of the interplanetary trajectories covering the 30 days of the Cassini launch period in October-November 1997 as well as the design of candidate orbital tours for the Cassini mission.

Galileo Orbital Tour

The current reference orbital tour described in Ref. 5 was designed with CATO as discussed in this paper. The process of designing the original version of this tour is described in detail in Ref. 6 and used the earlier optimization methods described in Ref. 1. This current version of the tour represents the final trajectory design prior to Jupiter arrival on December 7, 1995. Once the Galileo Orbiter is in orbit around Jupiter, CATO will be used at each opportunity for re-optimizing the tour based on updated information about the actual trajectory and the ephemerides and masses of the Galilean satellites and Jupiter itself.

Table 1 shows the position discontinuities (AR) at the breakpoints for the initial values of the control point variables used for the generation of this reference tour. It is seen that several of the values are nearly 100,000 km. Also shown arc the velocity discontinuities (ΔV) for the 4 breakpoints (the midpoints between two flybys on the same orbit) at which a AV is not allowed. These values range up to nearly 70 m/s. Not shown arc the velocity discontinuities for the other breakpoints that are not constrained to be zero. "l'hose initial values range from tens to hundreds of meters per second. In the optimization their sum will be minimized,

The control points include the flyby parameters (epoch, altitude, b-plane angle, time from closest approach and V_∞ vector) for each flyby, as well as an initial control point (epoch and Jupiter centered Cartesian state) between the. initial state and the large perijove raise maneuver (PJR) located near apojove of the initial orbit, Following the sixth targeted flyby (E6) and the ninth targeted flyby (C9), a Jupiter centered control point (using classical orbital elements) is used to constrain the Jovicentric inclination to achieve a distant occultation by the satellite 10, For each set of control point variables, those which arc fixed arc indicated with an (*).

Table 2 shows that for the converged solution all the breakpoint position discontinuities (AR*) and the velocity discontinuities for the 4 constrained breakpoints (AR*) are reduced to zero. The resultant unconstrained AV magnitudes at the other breakpoints are also shown, Of the 13 allowed AV's, it is seen that only three significant non-zero values result, All the others optimize to zero or nearly so. The converged solution is reached in only 4 iterations, The first iteration reduces the largest position mismatch from over 88,000 km to less than 1200 km and reduces the largest constrained velocity mismatch from over 66 m/s to 0.5 m/s, After the fourth iteration all the position discontinuities are less than 0.01 km and the velocity discontinuities are less than 1x10-s m/s. References 5 and 6 contain a detailed discussion of the characteristics of this trajectory.

Table 1

GALILEO ORBITAL TOUR REFERENCE TRAJECTORY - INITIAL BREAKPOINT DISCONTINUITIES AND CONTROL POINT PARAMETER SETS

Breakpoints		Control Points
OTM-2:	AR= 6,598 km	Pre-PJR Leg: $T^*, x, y, z, v_x, v_y, v_z$
PJR:	AR = 2,915 km	**Ganymede-1:** $T', H', \theta, t_p^*, V_\infty, \delta, \alpha$
Post G1 ape:	AR = 24,594 km	**Ganymede-2:** $T', H, \theta, t_p', V_\infty, \delta, \alpha$
Post G2 ape:	AR = 22,543 km	**Callisto-3:** $T^*, H, \theta, t_p^*, V_\infty, \delta, \alpha$
C3-E3A **mid:**	AR = 340 km ΔV = *3.844* m/s	**Europa-3A:** $T, H, \theta, t_p', V_\infty, \delta, \alpha$
Post C3 ape:	AR = 77,293 km	**Europa-4:** T^*, **II,** θ, t_p', V_∞, δ, α
Post E4 ape:	AR = 66,780 km	**Europa-5A:** $T, I\text{-}i, \theta, t_p', V_\infty, \delta, \alpha$
Orbit 5 ape:	AR = 56,953 km	**Europa-6:** $T, II, 0, t_p^*, V_\infty, \delta, \alpha$
E6 + 3 days:	AR = 2,962 km	Orb 6 **Io occul:** $1^*, a, e, i^*, \Omega, \omega, M$
Post E6 ape:	AR = 88,282 km	**Europa-7A:** **T,** $H, \theta, t_p^*, V_\infty, \delta, \alpha$
E7A-G7 mid:	ΔR = 1,919 km AV = 65.225 m/s	**Ganymede-7:** **1-,** $H, \theta, t_p', V_\infty, \delta, \alpha$
Post G7 ape:	AR = 37,034 km	**Callisto-8A:** $T, H, \theta, t_p', V_\infty, \delta, \alpha$
C8A-G8 mid:	AR = 1,488 km AV = 6.437 m/s	**Ganymede-8:** $T, H, \theta, t_p^*, V_\infty, \delta, \alpha$
Post G8 ape:	AR =61 ,869 km	**Callisto-9:** $T, H, \theta, t_p^*, V_\infty, \delta, a$
C9-G9A mid:	ΔR = 1,120 km AV = 12.139 m/s	**Ganymede-9A:** $T, H, \theta, t_p', V_\infty, \delta, \alpha$
C9 + 3 days:	AR = 7,027 km	**Orb 910 occul:** $T^*, a, e, i^*, \Omega, \omega, M$
Post C9 ape:	AR= 6,667 km	**Callisto-10:** $T, H, \theta, t_p', V_\infty, \delta, a$
Post C1O ape:	AR= 6,236 km	**Europa-n:** $T, H^*, \theta, t_p^*, V_\infty, \delta, \alpha$
Post El 1 ape:	AR= 9,380 km	**Europa-12:** $T^*, H^*, \theta, ^* t_p^*, V_\infty, \delta, \alpha$
Post E12 ape:	unconstrained	

In these tables the Galilean satellites are indicated by G, C, and E for Ganymede, Callisto and Europa respectively, The number indicates the orbit on which the flyby occurs *(i. e.,* C3 for Callisto on the third orbit) and in the case where two flybys occur on the same orbit, the more distant one (referred to as "non-targeted") is indicated with an "A" *(i.e.,* E3A for the non-targeted Europa on orbit 3).

Table 2

GALILEO ORBITAL TOUR REFERENCE TRAJECTORY - CONVERGED CONDITIONS

Breakpoints		
OTM-2:	AR'	AV = 0.00 m/s
PJR:	AR*	ΔV =3-75.42 m/s
Post G1 ape:	AR*	ΔV = 4.98 rrds
Post G2 ape:	AR*	ΔV = 0.00 m/s
C3-E3A mid:	AR'	AV*
Post C3 ape:	AR*	AV = 0.00 m/s
Post E4 ape:	AR*	AV = 0.00 m/s
Orbit 5 ape:	AR*	AV = 0.00 m/s
E6 + 3 days:	AR*	AV = 0.00 m/s
Post E6 ape:	AR*	AV = 16.00 m/s
E7A-G7 mid:	AR*	ΔV*
Post G7 ape:	AR'	ΔV = 0.00 m/s
C8A-G8 mid:	AR*	AV*
Post G8 ape:	AR'	AV = 0.00 m/s
C9-G9A mid:	AR*	ΔV*
C9 + 3 days:	AR*	AV = 0.00 m/s
Post C9 **ape:**	AR*	AV = *0.09* m/s
Post C1O ape:	AR*	AV = 0.00 m/s
Post **E11** ape:	ΔR*	AV = *0.02* m/s
Post E12 ape:	unconstrained	
TOTAL ΔV		396.51 m/s

Cassini Interplanetary Trajectory

The primary interplanetary trajectory for the Cassini mission to Saturn is known as a VVEJGA (Venus-Venus-Earth-Jupiter-Gravity-Assist) trajectory (Ref. 7). This trajectory launches from Earth on October 6, 199'/, flies by Venus on April 21, 1998, and again on June 20, 1999. Then after only 58 days flies by the Earth on August 16, 1999. On December 30, 2000, Jupiter is encountered, with arrival at Saturn on July 1, 2004. This arrival date was chosen to give the best observation opportunity of the distant satellite Phoebe on Saturn approach,

Table 3 shows the position discontinuities (AR) at the breakpoints for the initial values of the control point variables used for the generation of this interplanetary trajectory. It is seen that these discontinuities range up to more than 26 million kilometers. The control points include the injection parameters for the departure hyperbola from Earth

(epoch, altitude, b-plane angle, time of closest a]yx-each, energy, and asymptote direction), flyby parameters (epoch, altitude, b-plane angle, time of closest approach and V_∞ vector) for each planetary flyby, and the arrival hyperbola at Saturn (epoch, altitude, b-plane angle, time of closest approach and V_∞ vector). For each set of control point variables, those which are fixed are indicated with an (*), Table 4 indicates that for the converged solution all the breakpoint position discontinuities (ΔR^*) are reduced to zero. The resultant unconstrained AV magnitudes at the breakpoints are also indicated. Of the 5 AV's, it is seen that only the one on the Venus to Venus transfer leg is non-zero. All the others optimize to zero. This converged solution is also reached in only 4 iterations. The first iteration reduces the largest position mismatch from over 26,000,000 km to less than 770,000 km. After the fourth iteration all the position discontinuities are less than 0.1 km. Characteristics of the interplanetary transfer trajectories being considered for the Cassini mission arc discussed in Ref. 7.

Table 3

CASSINI INTERPLANETARY TRAJECTORY - INITIAL BREAKPOINT DISCONTINUITIES AND CONTROL POINT PARAMETER SETS

Breakpoints		Control Points	
Earth Departure:	unconstrained		
		Depart Hyp:	T*, Ii*, O', t_p^*, C_3, δ, α
Earth-Vi Man:	**AR = 110,058** km		
		Venus-1:	T, Ii', θ, t_p', V_∞, δ, α
V1-V2 Man:	AR = 2,546,780 km		
		Venus-2:	T, H, O, t_p^*, V_∞, δ, α
V2-Earth-2 Man:	AR = 632,873 km		
		Earth-2:	T, H', o, t_p', V_∞, δ, α
E2-Jupiter Man:	AR = 1,618,776 km		
		Jupiter:	1, t-l, θ, t_p', V_∞, δ, α
Jup-Saturn Man:	AR= 26,477,446 km		
		Arrival Hyp:	T*, H*, θ^*, t_p', V_∞, δ, *a*
Saturn Arrival:	unconstrained		

Table 4

CASSINI INTERPLANETARY TRAJECTORY - CONVERGED CONDITIONS

Breakpoints

Earth Departure: unconstrained		
Earth-Vi Man:	AR*	AV = 0.00 m/s
V1-V2 Man:	A R '	AV =466.19 m/s
V2-Earth-2 Man:	AR'	AV = 0.00 m/s
E2-Jupiter Man:	AR*	AV = 0.00 m/s
Jup-Saturn Man:	AR*	AV = 0.00 m/s
Saturn Arrival: unconstrained		
TOTAL AV		466.19 m/s

Cassini Saturn Orbit Insertion and Probe and Orbiter Trajectories to Titan

The interplanetary trajectory described above is the basis for this trajectory. The state vector at the breakpoint between Jupiter and Saturn is used as the initial state. The epoch of the first control point is chosen to be 1 day before Saturn closest approach, but it specifies osculating closest approach parameters (altitude of closest approach, b-plane angle and a closest approach time that is 1 day later) with both the altitude and time of closest approach being constrained. The following breakpoint is 1 day later with an impulsive model for the Saturn Orbit Insertion (S01) maneuver. 'I 'he next control point is set 1 day later and is specified as a Cartesian state with respect to Saturn since no constraints are required, The following breakpoint is approximately at apoapsis of the initial Saturn orbit and models the perichrone raise (PCR) maneuver as an impulse. The next control point applies to the Probe trajectory and specifies the Probe targets for entering the atmosphere of Titan. Note that since the next breakpoint will be before. this occurs, the very useful capability of allowing a control point to lie outside the time interval defined by the two breakpoints that precede and follow it, allows CATO to integrate the state defined by the (Probe) control point at Titan backwards in time to these breakpoints. The next breakpoint is the O-biter Deflection Maneuver (ODM), which is modeled as an impulse and applies to the Orbiter trajectory that will fly by Titan and on to the orbital tour of Saturn. The final control point specifies the Orbiter flyby parameters at Titan. As the Orbiter approaches and then flies by Titan it receives information from the Probe that is descending into Titan's atmosphere. Both the Probe and Orbiter control points use hyperbolic orbital elements with respect to Titan. Certain of these elements are constrained to achieve particular science objectives. The time difference between the two spacecraft at Titan is also constrained.

Table 5

CASSINI ORBIT INSERTION TRAJECTORY - INITIAL BREAKPOINT DISCONTINUITIES AND CONTROL POINT PARAMETER SETS

Breakpoints		Control Points	
Jup-Saturn Man:	AR = 1,575,842 km		
sol:	ΔR = 1,833 km	**Arrival Hyp:**	**T*, H*,** θ, t_p**',** V_∞, δ, α
PCR:	AR = 358,416 km	**Initial Orbit:**	**T',** x, y, z, v_x, **vy,** v_z
ODM:	AR = 24,422 km	**Probe Entry:**	**T*,** B^*, θ^*, **y',** V_∞, δ, α
T1-T2 ape:	**unconstrained**	**Titan-1 (Orb):**	T^*, **H', 0',** $t_p{}^*, V_\infty, \delta, \alpha$

Table 5 shows the position discontinuities (AR) at the breakpoints for the initial values of the control point variables used for the generation of this trajectory. It is seen that these discontinuities range up to more than 1.5 million kilometers. The control points are as described above and include a variety of flyby parameters. Table 6 indicates that for the converged solution all the breakpoint position discontinuities (AR*) are reduced to zero. The resultant unconstrained AV magnitudes at the breakpoints are also indicated.

Due to the highly constrained nature of this trajectory problem, only the initial **AV is** zero as would be expected. This solution is reached in 4 iterations as well, even though it is quite different in nature from the previous two. The first iteration reduces the largest position mismatch from over 1.5 million kilometers to less than 7,000 km. After the fourth iteration all the position discontinuities are less than 0.1 km.

Table 6

CASSINI ORBIT INSERTION TRAJECTORY - CONVERGED CONDITIONS

Breakpoints		
Jup-Saturn Man:	**AR***	AV = 0.00 m/s
sol:	AR'	AV =550.55 m/s
PCR:	AR*	AV = 321.20 m/s
ODM:	AR*	AV = 57.32 m/s
T1-T2 ape:	unconstrained	
TOTAL AV		929.08 m/s

Stardust Interplanetary Trajectory

The Stardust Mission is a proposed Discovery class mission that is designed to make a fast flyby of comet Wild-2 at a very close approach distance and return to Earth with samples of the dust and gas from the region close to the comet nucleus. The trajectory shown here leaves the Earth on February 15, 1999, on a AVEGA (Delta-V Earth Gravity Assist) trajectory that re-encounters the Earth on January 17, 2001, to gain sufficient heliocentric energy to encounter comet Wild-2 on January 1, 2004. This trajectory then returns to the Earth on January 17, 2006.

Table 7

STARDUST INTERPLANETARY TRAJECTORY - INITIAL BREAKPOINT DISCONTINUITIES AND CONTROL POINT PARAMETER SETS

Breakpoints		Control Points	
Earth Departure:	**unconstrained**		
		Depart Hyp:	**T*, H*,** θ^*, t_p^*, **C3,** δ, α
DVEGA Man:	**AR = 3,012,408 km**		
		Earth Flyby:	T, H, θ, t_p', V_∞, δ, α
W2 Approach:	AR= 4,518,531 km		
		Wild-2:	$T^*, x^*, y^*, z^*, v_x, v_y, v_z$
W2-Earth Ret:	AR= 408,094 **km**		
		Arrival Hyp:	**T', H*,** $\theta^*, \gamma^*, V_\infty, \delta, \alpha$
Earth Arrival:	unconstrained		

Table 7 shows the position discontinuities (AR) at the breakpoints for the initial values of the control point variables used for the generation of this trajectory. It is seen that these discontinuities range up to more than 4.5 million km. These control points include the flyby parameters (epoch, altitude, b-plane angle, time of closest approach and V_∞ vector) for the planetary and comet flybys as well as the Earth departure and arrival parameters. Table 8 indicates that for the converged solution all the breakpoint position discontinuities (ΔR^*) are reduced to zero. The resultant unconstrained AV magnitudes at the breakpoints are also indicated, Due to the various constraints, all the AV's are non-zero for this case. This solution is reached in 6 iterations. The first iteration reduces the largest mismatch to about 750,000 km, but the next iteration reduces it to less than 2,000 km. After the sixth iteration all the position discontinuities are less than 0.1 km.

Table 8

STARDUST 1NTERPLANETAR% TRAJECTORY - CONVERGED CONDITIONS

Breakpoints		
Earth Departure: unconstrained		
DVEGA Man:	**AR***	**AV = 179.10 m/s**
W2 Approach:	AR'	**AV = 64.50** m/s
W2-Earth Ret:	**AR***	AV = 1.7'3 m/s
Earth Arrival:	**unconstrained**	
TOTAL AV		245.33 m/s

SUMMARY AND CONCLUSION

A new and very effective method for optimizing complex multi-flyby trajectories has been implemented and applied to a number operational and proposed missions. The initial applications have proven quite successful, with the computer program being easy to use and demonstrating quite robust convergence properties.

ACKNOWLEDGMENT

The research described in this paper was carried out by the Jet Propulsion Laboratory, California Institute of l'ethnology, under a contract with the National Aeronautics and Space Administration. We would like to thank Sylvia Miller and Jess Fordyce for their help and continued support during this effort. We would also like to thank Ted Sweetser and Chen-Wan Yen for their help in testing prototype versions of CATO and many useful comments for the final version, We are most grateful for the efforts of Ed Rinderle in the development of the very efficient integration routines used by CATO as well as for his helpful and very useful comments during the development. Discussions with Fred Krogh and John Michael about the use of Chuck Lawson's linear weighted least squares routine and constrained optimization in general were most helpful. Finally, the help of Steve Flanagan in the implementation and testing of the launch and arrival body code was invaluable.

REFERENCES

1. D'Amario, L. A., Byrnes, D, V., and Stanford, R. H., "A New Method for Optimizing Multiple-Flyby Trajectories," *Journal of Guidance, Control, and Dynamics*, Vol. 4, *No. 6,* November-December 1981, pp. 591-596.

2. D'Amario, L. A., Byrnes, D, V., and Stanford, R. H., "Interplanetary Trajectory Optimization with Application to Galileo," *Journal of Guidance, Control, and Dynamics,* Vol. 5, No. 5, September-October 1982, pp. 465-471.

3. Ishii, N. and Matsuo, H., "Design Procedure of Accurate Orbits in a Multi-Body Frame with a Multiple Swingby," AAS Paper 93-655, AAS/AIAA Astrodynamics Conference, Victoria, B. C., August 1993.

4. Carrico, J., Hooper, H. L., and Roszman, L., "Rapid Design of Gravity Assist Trajectories," 3rd International Symposium on Spacecraft Flight Dynamics, Darmstadt, Germany, 30 September -4 October, 1991.

5. D'Amario, L. A., Byrnes, D. V., Haw, R. J., Kirhofer, W. E., Nicholson, F. T., Wilson, M. G., "Navigation Strategy for the Galileo Jupiter Encounter and Orbital Tour," A AS Paper 95-381, AAS/AIAA Astrodynamics Conference, Halifax, Nova Scotia, Canada, August 1995.

6. Wolf, A. A.. and Byrnes, D. V., "Design of the Galileo Satellite Tour," AAS Paper 93-567, AAS/AIAA Astrodynarnics Conference, Victoria, B. C., August 1993.

7. Flanagan, S. and Peralta, F., "Cassini 1997 VVEJGA Trajectory Launch/Arrival Space Analysis," AAS Paper 93-684, AAS/AIAA Astrodynamics Conference, Victoria, B. C., August 1993.